

Strong Quantum Mpemba Effect with Squeezed Thermal Reservoirs

J. Furtado 

Centro de Ciências e Tecnologia, Universidade Federal do Cariri, 63048-080, Juazeiro do Norte, Ceará, Brazil

E-mail: job.furtado@ufca.edu.br

Alan C. Santos 

Instituto de Física Fundamental, Consejo Superior de Investigaciones Científicas, Calle Serrano 113b, 28006 Madrid, Spain

E-mail: ac_santos@iff.csic.es

Abstract. The phenomena where a quantum system can be exponentially accelerated to its stationary state has been refereed to as Quantum Mpemba Effect (QMpE). Due to its analogy with the classical Mpemba effect, *hot water freezes faster than cold water*, this phenomena has garnered significant attention. Although QMpE has been characterized and experimentally verified in different scenarios, sufficient and necessary conditions to achieve such a phenomenon are still under investigation. In this paper we address a sufficient condition for QMpE through a general approach for open quantum systems dynamics. With help of the *Mpemba parameter* introduced in this work to quantify how strong the QMpE can be, we discuss how our conditions can predict and explain the emergence of weak and strong QMpE in a robust way. As application, by harnessing intrinsic non-classical nature of squeezed thermal environments, we show how strong QMpE can be effectively induced when our conditions are met. Due to the thermal nature of environment considered in our model, our work demonstrates that a *hot qubit freezes faster than a cold qubit* only in presence of squeezed reservoirs. Our results provide tools and new insights opening a broad avenue for further investigation at most fundamental levels of this peculiar phenomena in the quantum realm.

1. Introduction

Two physical systems initially at different temperatures, the cold T_c and hot $T_h > T_c$, are cooled down by exchanging energy with a colder reservoir at temperature $T_0 < T_c$. Even under the same cooling conditions, the hot system can reach regime of temperatures smaller than the cold system does during the process. This unconventional effect was observed in the classical physics realm by a 13 years old high school student, called Erasto B. Mpemba, in 1963. The experimental verification of the effect was reported by E. B. Mpemba and D. G. Osborne in 1969 [1]. F. Carollo *et al* [2] introduced a mechanism able to exponentially speed up the dynamics of a quantum system to the stationary state, which can be interpreted as a

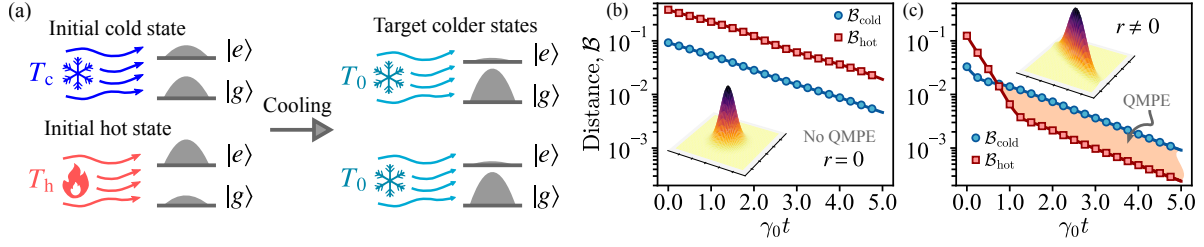


Figure 1. (a) Two identical two-level systems are prepared initially in thermal states at different temperatures T_c and T_h . The systems are cooled down independently to a target colder temperature $T_0 < T_c$. During the cooling process the population of the excited states $|e\rangle$ of each system is transferred to the ground state $|g\rangle$. The emergence of QMpE depends on the squeezing parameter r of the bath, where (b) QMpE is not observed in our model for Gaussian thermal baths ($r = 0$), but (c) by considering non-zero squeezing parameters, the QMpE is engineered.

Mpemba's effect in the quantum realm. Since then, such a quantum Mpemba's effect (QMPE) has aroused further investigations about the phenomena and its characterization in different contexts [3, 4, 5, 6, 7, 8, 4, 9, 10, 11, 12, 13, 14].

The QMpE has been investigated in the context of Markovian dynamics of many-body systems through Dicke model [2], Anderson model (quantum dots reservoirs) [3], Lieb-Liniger model [4], and spin chain systems [5, 6] for example. However, to the best of our knowledge, the first experimental evidence of such an effect was done recently by J. Zhang *et al* [15] in a single trapped ion systems, exploiting the dynamics of tree-level system encoded in the low-lying electronic states of a trapped $^{40}\text{Ca}^+$ ion. However, all these works, among others [8, 4, 9], have considered the interaction of the physical system with reservoirs described by physical processes other than that one observed in thermal reservoirs with well defined finite temperature ($T > 0$). To deal with the proper measure and characterization, some authors [3, 10] have considered the definition of an alternative version of temperature for isothermal processes, where detailed study on the exchanged heat and entropy variation of the system is considered.

As depicted in Fig. 1a, a genuine QMpE should be possible if the initial hot and cold states are prepared using the same reservoir at different temperatures, and then use the same bath at a colder temperature to induce the QMpE. In addition, despite efforts to observe and characterize the QMpE, the specific conditions required to induce this effect and the mechanism behind it remain to be explored in greater detail. In this regard, we address these two questions. Firstly, we conveniently exploit the theory of open quantum system in the superoperator formalism to derive fundamental conditions that should be satisfied to efficiently achieve QMpE [16]. Such conditions are then used to show that, in the context of reservoir, Hamiltonian and state preparation engineering, they provide a consistent way of explaining the mechanism behind the emergence of QMpE. With help of a fidelity-base figure of merit introduced in this work, as shown in Figs. 1b and 1c, we identify the emergence of thermally induced QMpE in a two-level atom interacting with squeezed thermal reservoirs. In addition to the application of squeezed in gravitational-wave detection [17, 18, 19], quantum

metrology [20, 21], efficient quantum thermal engines [22, 23, 24, 25], among others [26], our work establishes the impact of squeezed thermal baths to reached out genuine QMpE.

2. Sufficient conditions for QMpE

First of all, let us introduce a function (or quantifier) used as a figure of merit (or witness) of the Mpemba's effect. Such a function is defined from the measure of the distance (or infidelity) between two quantum states, introduced in context of quantum information [27], obtained from the trace distance $\mathcal{B}_{c,h}(t) = \|\hat{\rho}_{c,h}(t) - \hat{\rho}_0\|_1$, with $\|\hat{A}\|_1 = [\text{Tr}(\hat{A}^\dagger \hat{A})]^{1/2}$. $\hat{\rho}_c(t)$ and $\hat{\rho}_h(t)$ are solutions of the Lindblad equation for the initial condition $\hat{\rho}_c(0) = \hat{\rho}_c$ and $\hat{\rho}_h(0) = \hat{\rho}_h$, respectively. From this equation, and with help of Figs. 1b and 1c, it is possible to state that whenever the initial states satisfy $\mathcal{B}_h(0) > \mathcal{B}_c(0)$, the Mpemba's effect is observed when $\mathcal{B}_h(t) < \mathcal{B}_c(t)$, as \mathcal{B} quantifies the distance to the steady state. Therefore, we define the infidelity-based quantity

$$\mathcal{M}_{\mathcal{B}} = \frac{\mathcal{A}_{\mathcal{B}_c > \mathcal{B}_h}}{\mathcal{A}_{\mathcal{B},0}} = \frac{\frac{1}{\tau} \int_{\mathcal{B}_c > \mathcal{B}_h} |\mathcal{B}_c(t) - \mathcal{B}_h(t)| dt}{\frac{1}{\tau} \int_0^\tau |\mathcal{B}_c(t) - \mathcal{B}_h(t)| dt}. \quad (1)$$

The function $\mathcal{A}_{\mathcal{B}_c > \mathcal{B}_h}$ quantifies the (time-averaged) contributions of the fidelity when the hot state gets closer to the target state in comparison to the colder one (as sketched in Fig. 1b). On the other hand, $\mathcal{A}_{\mathcal{B},0}$ quantifies the time average of the absolute value of the difference between the $\mathcal{B}_c(t)$ and $\mathcal{B}_h(t)$ during the total evolution time τ . By construction, \mathcal{M} has to be smaller than 1, as the initial condition of our problem we have to choose quantum states such that $\mathcal{B}_c(0) < \mathcal{B}_h(0)$, as depicted in Fig. 1. Also, it is possible to observe that the integral function will capture any contribution of the dynamics in which $\mathcal{A}_{\mathcal{B}_c > \mathcal{B}_h}$, such that $\mathcal{M} > 0$ indicates the emergence of the Mpemba's effect within the integration interval considered. Since the absence of Mpemba's effect leads to $\mathcal{M} = 0$, we can conclude that our parameter obeys $0 \leq \mathcal{M} < 1$. In this way, the bigger the parameter \mathcal{M} , the stronger the Mpemba's effect.

Now we introduce new conditions for the emergence of the QMpE through the superoperator formalism for quantum open systems. To this end, our starting point is a time-local Master equation of a quantum system of the form

$$\frac{d}{dt} \hat{\rho}(t) = \mathfrak{L}[\hat{\rho}(t)], \quad (2)$$

where $\hat{\rho}(t)$ is the system master equation and $\mathfrak{L}[\bullet]$ is the dynamics generator in the system's Hilbert space \mathcal{H} , which encodes the information about the dynamics when the system interacts with external fields and its surroundings, for example. One alternative way to rewrite the above equation, and convenient to our discussion, is through the *superoperator formalism* [16, 28, 29, 30, 31] (see Appendix A for further details). In fact, through this formalism the Eq. (2) can be rewritten in a "Schrödinger form" as [16]

$$|\dot{\varrho}(t)\rangle\rangle = \mathbb{L}|\varrho(t)\rangle\rangle, \quad (3)$$

where $|\varrho(t)\rangle\rangle$ is the *coherence vector* associated to the density matrix $\hat{\rho}(t)$ with components given by $\varrho_n(t) = \text{tr}[\rho(t)\sigma_n^\dagger]$, for a basis $\{\sigma_n^\dagger\}$ of D^2 operators $\sigma_n^\dagger \in \mathcal{H}$, with $D = \dim[\mathcal{H}]$.

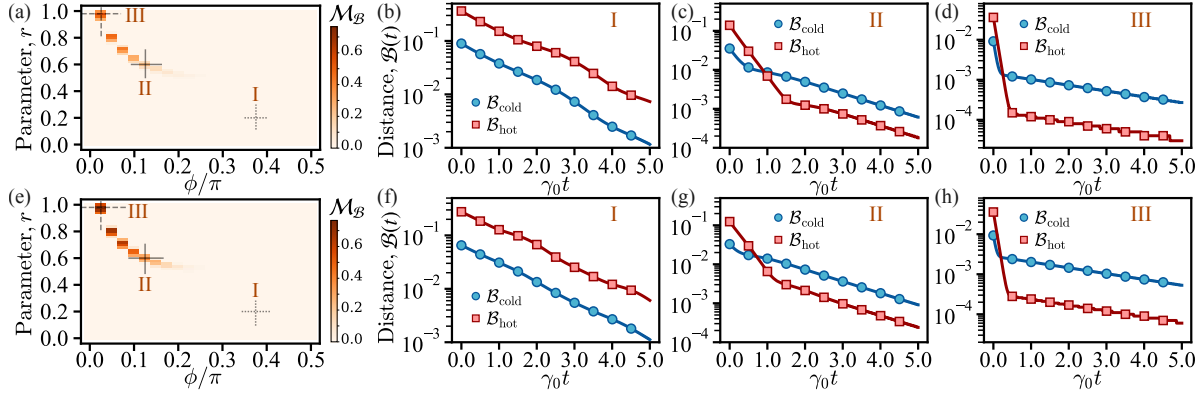


Figure 2. Mpemba parameter M_B as function of the squeezing degree r and the external driving phase ϕ for (a) $\Omega/\Delta_0 = 0.5$ and (b) $\Omega/\Delta_0 = 1.0$. The distance between the hot and cold states with respect to the coldest steady state is shown in (c,d,e) for the highlighted points I, II and III of (a), respectively. Similarly, the distance shown in (c,d,e) is related to the highlighted points I, II and III of (b), respectively. The temperature for the initial states is considered as $\hbar\omega_0/T_c k_B = 2.0$ and $\hbar\omega_0/T_h k_B = 0.1$ for the cold and hot states, and $\hbar\omega_0/T_0 k_B = 100$ for the coldest target state. We set the squeezing phase $\varphi = 0$.

Similarly, using the same basis we can define \mathbb{L} as a $D^2 \times D^2$ operator with matrix elements $\mathbb{L}_{kn} = \text{tr}[\sigma_k^\dagger \mathcal{Q}[\sigma_n]]$, the *super-operator Lindbladian*. In this way, it is possible to observe that any information about the dynamics generator and the system state are now encoded in \mathbb{L} and $|\varrho(t)\rangle\rangle$, respectively. As consequence of this formalism, we can write the solution for the system dynamics as $|\varrho(t)\rangle\rangle = e^{\mathbb{L}t}|\varrho(0)\rangle\rangle$. This formalism is convenient to our discussion because we can write the solution $|\varrho(t)\rangle\rangle$ as a linear decomposition of the left- and right-eigenvectors of \mathbb{L} . In fact, without loss of generality, let us assume the set of left- and right-eigenvectors of \mathbb{L} satisfying $\mathbb{L}|\mathcal{R}_n\rangle\rangle = \lambda_n|\mathcal{R}_n\rangle\rangle$ and $\langle\langle\mathcal{L}_n|\mathbb{L} = \lambda_n\langle\langle\mathcal{L}_n|$, respectively, then one gets (see [Appendix B](#) for further details)

$$|\varrho(t)\rangle\rangle = \sum_{n=0}^{D^2-1} e^{\lambda_n t} \gamma_n |\mathcal{R}_n\rangle\rangle. \quad (4)$$

with coefficients $\gamma_n = \langle\langle\mathcal{L}_n|\varrho(0)\rangle\rangle$. Therefore, we have now shown that the dynamics of the coherence vector is uniquely obtained by the initial state and the spectrum of \mathbb{L} . In this way, we can now study the expected behavior of the system in the steady-state, as well as the relevant decay rates of interest to emergence of the Mpemba effect.

First of all, it is worth to state that the classical and quantum versions of the Mpemba effect only depends on the initial states of the hot and cold system, and the common environment used to cooling down the systems independently. Within the framework considered here for the QMpE, this means that the hot and cold systems have initial states represented by different coherence vectors, say $|\varrho_c(0)\rangle\rangle$ and $|\varrho_h(0)\rangle\rangle$, respectively, but they are driven through the same super-operator Lindbladian, and therefore we can write down

$$|\varrho_{c/h}(t)\rangle\rangle = \sum_{\text{Re}[\lambda_n]=0} e^{\lambda_n t} \gamma_n^{c/h} |\mathcal{R}_n\rangle\rangle + \sum_{\text{Re}[\lambda_n] \neq 0} e^{\lambda_n t} \gamma_n^{c/h} |\mathcal{R}_n\rangle\rangle. \quad (5)$$

where we already separated the sum into two parts associated to all eigenvalues λ_n with $\text{Re}[\lambda_n] = 0$, and $\text{Re}[\lambda_n] \neq 0$. The physical intuition behind this distinction relies on the

fact that the first term of the above equation may describe the existence of one or multiple steady states, and the second term vanishes for sufficiently large evolution time.

In context of QMpE, the main conclusion of Eq. (5) can be interpreted as follows. By ordering the eigenvalues such that $\text{Re}[\lambda_0] \geq \text{Re}[\lambda_1] \geq \dots \geq \text{Re}[\lambda_{D^2-1}]$, the component of $|\varrho_{c/h}(t)\rangle\rangle$ associated to $\text{Re}[\lambda_{D^2-1}]$ will decay much faster than the component of $\text{Re}[\lambda_1]$. It means that a hot state obeying $|\gamma_1^h| \leq |\gamma_2^h| \leq \dots \leq |\gamma_{D^2-1}^h|$ should approach the steady state faster than a cold state with $|\gamma_1^c| \geq |\gamma_2^c| \geq \dots \geq |\gamma_{D^2-1}^c|$. In addition to these conditions, it is also relevant to observe the relation between the coefficients associated to the eigenvalue most negative real part λ_{D^2-1} and the first eigenvalue with a non-zero real part, say λ_x , such that $\text{Re}[\lambda_x] < 0$. According to Eq. (5), one expects to be able to observe strong QMpE if the additional relations $|\gamma_{\lambda_{D^2-1}}^h| \geq |\gamma_{\lambda_{D^2-1}}^c|$ and $|\gamma_{\lambda_x}^h| \leq |\gamma_{\lambda_x}^c|$, between the cold and hot initial states is satisfied.

Notice that, differently from Ref. [4], we are not providing conditions to *characterize* QMpE (this is done through the parameter \mathcal{M}), the inequalities stated are expected to be satisfied for any hot and cold states in which the QMpE can be *reached out*. Of course, since an analytical solution of $|\varrho_{c/h}(t)\rangle\rangle$ for an arbitrary dynamics is impossible, the degree of rigor of our approach only allows to state that these conditions are *necessary*, but *not sufficient* for QMpE. It means that, the absence of QMpE can be observed even when satisfying these inequalities, but it is not expected to observe QMpE if such conditions are not satisfied. Now, the relevance and applicability of these conditions will be discussed in a concrete example.

3. QMpE with squeezed thermal baths

The system of interest in this work is a single quantum two-level system interacting with a *squeezed thermal bath*, at temperature T . Such a kind of reservoir is efficiently engineered in the current state-of-the-art in nanobeam experiments with squeezed electronic noise [22], or in optical cavity systems [32, 33, 34]. As a model, such a system is described by the total Hamiltonian $\hat{H}_T = \hat{H}_{\text{tls}} + \hat{H}_b + \hat{H}_{\text{int}}$. We assume that the two-level system has generic excited and ground states, respectively denoted by $|e\rangle$ and $|g\rangle$, such that $\hat{H}_{\text{tls}} = \hbar\omega_0(|e\rangle\langle e| - |g\rangle\langle g|)$. The thermal bath is described by a system of non-interacting quantum Harmonic oscillators as $\hat{H}_b = \hbar \sum_k \omega_k \hat{b}_k^\dagger \hat{b}_k$, and the bath interacts with the two-level system through the interaction Hamiltonian

$$\hat{H}_{\text{int}} = \hbar \sum_k g_k \left[(\hat{\sigma}^+ + \hat{\sigma}^-) \hat{b}_k + \hat{b}_k^\dagger (\hat{\sigma}^+ + \hat{\sigma}^-) \right], \quad (6)$$

where $\hat{\sigma}^+ = (\hat{\sigma}^-)^\dagger = |g\rangle\langle e|$, and g_k is the coupling of the atom with the bath mode with wave vector k . The reservoir temperature and squeezing properties are introduced by assuming each mode of the reservoir initially at the state $\hat{\rho}_{b,k}(0) = \hat{S}_k(r, \varphi) \hat{\rho}_{b,k}^{\text{th}}(0) \hat{S}_k^\dagger(r, \varphi)$, where $\hat{\rho}_{b,k}^{\text{th}}(0)$ is the thermal state of the bath modes at temperature T , and $\hat{S}_k(r, \varphi) = \exp[\frac{1}{2} \xi_k^* \hat{b}_k^2 - \text{h.c.}]$ is the squeezing operator, with the squeezing parameters r_k and φ_k encoded in $\xi_k = r_k e^{i\varphi_k}$ [35]. For simplicity, we assume $\xi_k = \xi = r e^{i\varphi}$ for all k . Under these conditions, the dynamics for the

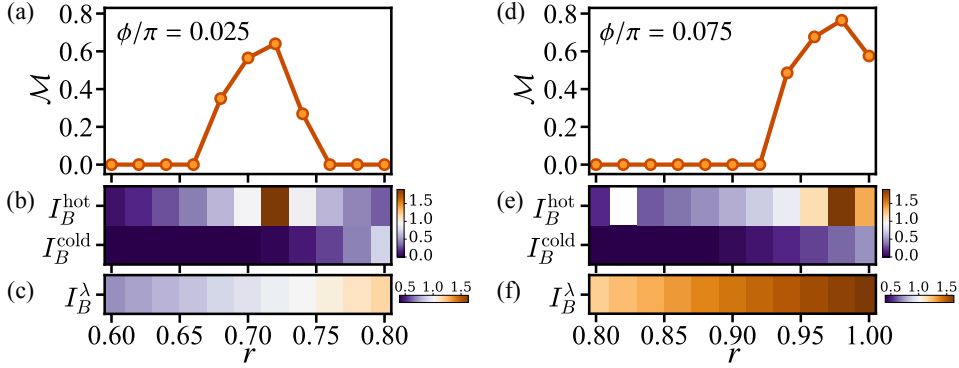


Figure 3. Synchronized behavior for the parameter \mathcal{M} , the ratio between the populations of the coldest reservoir modes in the hot I_B^{hot} and cold I_B^{cold} initial states, and the ratio I_B^λ between the highest and lowest relaxation decay as function of the squeezing parameter r . The quantities I_B^{hot} , I_B^{cold} , and I_B^λ are measured in units of Bel.

two-level system is governed by Eq. (2), with the effective Lindblad superoperator $\mathfrak{L}[\bullet]$ as

$$\mathfrak{L}[\bullet] = \frac{1}{i\hbar}[\hat{H}_{\text{tls}}, \bullet] + \frac{1}{2} \sum_{n=1}^2 [2\hat{R}_n \bullet \hat{R}_n^\dagger - \{\hat{R}_n^\dagger \hat{R}_n, \bullet\}], \quad (7)$$

with $\hat{R}_1 = \sqrt{\gamma_0(N_{\text{th}} + 1)}\hat{R}(r, \varphi)$, and $\hat{R}_2 = \sqrt{\gamma_0 N_{\text{th}}}\hat{R}^\dagger(r, \varphi)$, where $\hat{R}(r, \varphi) = \cosh(r)\hat{\sigma}^- + e^{i\varphi} \sinh(r)\hat{\sigma}^+$, $\hat{\sigma}^- = \hat{\sigma}^{+\dagger} = |g\rangle\langle e|$, γ_0 the spontaneous emission rate, and we assume the Bose-Einstein statistics for the average number of thermal photons $N_{\text{th}} = 1/(e^{\hbar\omega_0/k_B T} - 1)$. The above dynamics is valid under the Born-Markov and rotating wave approximations [36, 37].

In this framework, the hot and cold initial states $\hat{\rho}_h$ and $\hat{\rho}_c$ are prepared *independently* as the steady-state of the Eq. (7) for different temperatures T_h and T_c , respectively, for a given predefined set of squeezed parameters $\{r, \varphi\}$. In both cases, the Hamiltonian for the two-level system is the same, and we consider it as given by the Landau-Zener

$$\hat{H}_{\text{LZ}} = \hbar\Delta_0\hat{\sigma}^+\hat{\sigma}^- + \hbar\Omega(e^{i\phi}\hat{\sigma}^+ + e^{-i\phi}\hat{\sigma}^-). \quad (8)$$

which can be implemented by a weak classical oscillating drive ($\Omega \ll \omega_0$) with frequency ω_{dr} and phase ϕ , and detuned of $\Delta_0 = \omega_{\text{dr}} - \omega_0$ from the atomic transition ω_0 . After this stage, each system is placed in contact with the reservoir at very low temperature $Tk_B \ll \hbar\omega_0$, but keeping the same squeezing parameters used to prepare the hot and cold states, such the system is driven from their respective initial states according to the Eq. (7).

In Fig. 2 we show the behavior of the Mpemba parameter \mathcal{M} as function of the squeezing parameter r and the phase φ , for two different choices of ratio Ω/Δ_0 , and the behavior of the quantities $\mathcal{B}_c(t)$ and $\mathcal{B}_h(t)$ along the evolution for each initial state. As conclusion, it is possible to conclude that the QMpE is not a common effect in the system, as it is only possible to observe it for a small range of parameters. In particular, we highlight the case in which $r = 0.98$ and $\phi/\pi = 0.025$, where the parameter \mathcal{M} captures moderate and strong Mpemba effects in Fig. 2a and 2b, respectively. In fact, the Figs. 2c, 2d and 2e corresponds, respectively, to the points I, II and III of Fig. 2a, where one clearly observes that the parameter \mathcal{M} captures how strong the QMpE is for each case. Furthermore, of particular

interest we highlight the panels in Figs. 2f, 2g and 2h, related to the same points in Fig. 2b. By focusing on the cases II and III we can see that the QMpE gets stronger than in Fig. 2a, and it is mainly related to a faster decay of the hot state in both cases, while the cold states decay slower, leading then to a strong QMpE [15].

While the results aforementioned illustrate the role of the parameter \mathcal{M} introduced in this work, it does not explain anything about the QMpE. To this end, we now discuss how the conditions established previously allows us to understand the mechanism behind QMpE. To this end, we conveniently define some quantities to support our analysis. In this case, we know the system admits four eigenvalues λ_n , and then we define the quantity $I_B^\lambda = \log_{10}(\text{Re}[\lambda_3]/\text{Re}[\lambda_1])$, which provide the ratio between the real part of the fastest decay mode λ_3 and the slowest mode λ_1 in a Bel scale. This quantity is relevant to our analysis because I_B^λ quantifies how many orders of magnitude bigger $\text{Re}[\lambda_3]$ is compared with $\text{Re}[\lambda_1]$. Concomitantly, we claim that the QMpE can only be fully understood if we also investigate the relations between the populations γ_n for hot and cold states. Therefore, similarly, we also compute the same quantity defined for the “populations” γ_n of the hot and cold states. Of interest to our analysis is the ratio between $I_B^{\text{hot}} = \log_{10}(\text{Re}[\gamma_3^{\text{hot}}]/\text{Re}[\gamma_1^{\text{hot}}])$ and $I_B^{\text{cold}} = \log_{10}(\text{Re}[\gamma_3^{\text{cold}}]/\text{Re}[\gamma_1^{\text{cold}}])$. Therefore, we can now explain the emergence of strong Mpemba effect in the system.

In Fig. 2 we consider the set of parameters corresponding to the points III of the Figs. 2a and 2b. First we show, for each case, how \mathcal{M} changes with respect to the squeezing parameter r , and we observe that the highest values of \mathcal{M} in each example is achieved for different choices of r . This is the ideal scenario to test our conditions, so we investigate this behavior taking into account the Fig. 3. By increasing the squeezing parameter r , we create more squeezed thermal photons in the system, which directly affects the ratio I_B^λ . In principle, one could expect emergence of QMpE in for any $r > 0.7$, because we have QMpE for $r = 0.7$ and the decay rate of the mode λ_3 becomes even faster as r increases. However, this analysis fails in our system because the slowest decaying mode is significantly populated with respect to the other modes. Therefore we invoke the additional conditions over $|\gamma_n^{\text{hot}}|$ to explain this result.

In Figs. 3a, 3b and 3c we observe that even when $|\gamma_{3,2}|$ is around one order of magnitude bigger than $|\gamma_1|$, the Mpemba parameter detect a moderate QMpE because the population in the mode λ_1 is big enough to suppress QMpE. However, by combining the fact that $|\gamma_{3,2}| \gg |\gamma_1| > 0$, as seen in Fig. 3b, and $I_B^\lambda \sim 1$ ($\text{Re}[\lambda_3] \sim 10\text{Re}[\lambda_1]$), in Fig. 3c, we observe the maximum QMpE for the regime of parameters considered is achieved when $|\gamma_{3,2}| \gg |\gamma_1|$. In addition, this effect can be even stronger (strong QMpE) if we properly choose the Hamiltonian parameters from $\phi = 0.025\pi$ to $\phi = 0.075\pi$ (Figs. 3a, 3b and 3c), with \mathcal{M} reaching values close to 0.75. Similarly, our analysis explains the absence of QMpE even for the squeezed degree providing decay rates satisfying $\text{Re}[\lambda_3] \gg \text{Re}[\lambda_1]$. This result is relevant to our discussion because the Hamiltonian parameters can be efficiently controlled through external classical drives. In particular, we notice that in the regime in which QMpE is suppressed, such suppression is related to the fact that the hot state has a significant amount of population in the mode λ_1 . When such a population is sufficiently reduced, we can achieve

strong QMpE with $\mathcal{M} \approx 0.75$. It is worth to pay attention to the fact that, in all cases considered in Fig. 3, I_B^{cold} is small compared to I_B^{hot} , which reinforces our claim that the conditions established are *necessary* to achieve strong QMpE.

4. Conclusions and prospects

In conclusion, the results of our work are three-fold. First, we introduced a new parameter to efficiently witness the emergence of QMpE and to quantify how strong the QMpE is. Using this metric as figure of merit, we developed conditions able to predict scenarios where strong QMpE can be observed. Also, we showed how our results can be applied to explain the experimental observation of strong QMpE reported in Ref. [15]. To end, we also showed how to achieve different regimes of QMpE through of a single two-level system interacting with a squeezed thermal reservoir.

We state that the QMpE superoperator theory and conditions developed in this study goes beyond the example considered in this study. For example, our results shade light over the experimental results reported in Ref. [15]. In this work the authors provided experimental data for the eigenmodes of the Lindbladian of a three-level system encoded in the electronic states of a rapped $^{40}\text{Ca}^+$ ion. By driving such a system through the natural decay relaxation of the system, they investigate the behaviors of the populations of the cold and hot states with respect to the eigenmodes of $\mathcal{V}[\bullet]$ (slightly different from our definition). As conclusion, they engineered an initial (pure) strong QMpE state $|sME\rangle$ able to induce a very fast decay of the hot state in comparison with the cold one. As a characteristic of such a state, through the experimental data, they observed that the component of $|sME\rangle$ over the slowest decaying state is numerically zero. This corresponds to the discussions done for the results shown in Fig. 3 of our work.

It is worth to mention that, as aforementioned, our results can be experimentally reproduced in any experiment where squeezed thermal baths can be created or simulated. In particular, simulations of our findings can be done by digitizing the master equation considered in this work through squeezed Generalized Amplitude Damping channels [38]. In this regard, our results may be an sufficient, but not necessary, guide to describe both the reservoir and state engineering required to exploit new degrees of QMpE beyond the strong regime.

Acknowledgements

JF would like to thank the Fundação Cearense de Apoio ao Desenvolvimento Científico e Tecnológico (FUNCAP) under the grant PRONEM PNE0112-00085.01.00/16 for financial support, and the Conselho Nacional de Desenvolvimento Científico e Tecnológico (CNPq) under the grant 304485/2023-3. ACS acknowledges the support by the European Union's Horizon 2020 FET-Open project SuperQuLAN (899354), and by the Proyecto Sinérgico CAM 2020 Y2020/TCS-6545 (NanoQuCo-CM) from the Comunidad de Madrid.

Appendix A. Mathematical framework: Superoperator Formalism

In this section we review some fundamental mathematical tools of interest to our development. In particular, we discuss how to obtain: 1) The superoperator representation from the Lindblad and density matrix representation; and 2) The scheme to recover the density matrix representation from the superoperator formalism.

Appendix A.1. The superoperator formalism

Our discussion is mainly derived from Refs. [28, 16, 29, 39]. First of all, we adopt a *traceless* matrix basis $\{\sigma_1, \sigma_2, \dots, \sigma_{D^2-1}\}$ that satisfies $\text{tr}[\sigma_n \sigma_m^\dagger] = D\delta_{nm}$, the density matrix can be written as

$$\rho = \frac{1}{D} \left[\mathbb{1} + \sum_{n=1}^{D^2-1} \varrho_n \sigma_n \right] \quad (\text{A.1})$$

with $\varrho_n = \text{tr}[\rho \sigma_n^\dagger]$ and D the dimension of the Hilbert space. As an example, for a single qubit we assume such a basis as given by the set of the Pauli matrices

$$\sigma_1 = \sigma_x = \begin{bmatrix} 0 & 1 \\ 1 & 0 \end{bmatrix}, \quad \sigma_2 = \sigma_y = \begin{bmatrix} 0 & -i \\ i & 0 \end{bmatrix}, \quad \sigma_3 = \sigma_z = \begin{bmatrix} 1 & 0 \\ 0 & -1 \end{bmatrix}, \quad (\text{A.2})$$

where $\sigma_0 = \mathbb{1}$. In this way, the set of Pauli matrices can be used as a matrix basis for a two-level system and we write

$$\rho = \frac{1}{2} \left[\mathbb{1} + \sigma_x \varrho_x + \sigma_y \varrho_y + \sigma_z \varrho_z \right] = \frac{\mathbb{1} + \vec{\varrho} \cdot \vec{\sigma}}{2}, \quad (\text{A.3})$$

where we define the matrix Pauli vector $\vec{\sigma} = \sigma_x \hat{i} + \sigma_y \hat{j} + \sigma_z \hat{k}$, with $\{\hat{i}, \hat{j}, \hat{k}\}$ being the canonical basis of the \mathbb{R}^3 Euclidean space, and the *coherence vector* $\vec{\varrho} = \varrho_x \hat{i} + \varrho_y \hat{j} + \varrho_z \hat{k}$ for a two-level system.

Without loss of generality, here we consider the class of evolution where the system dynamics is described by the time-local master equation [30, 31]

$$\dot{\rho}(t) = \mathfrak{L}[\rho(t)], \quad (\text{A.4})$$

where $\mathfrak{L}[\bullet]$ is the generator of the dynamics of the system interacting with the environment. Thus, if we substitute $\rho(t)$ into Eq. (A.4) by using the expanded form of the Eq. (A.1), we find the system of differential equations

$$\dot{\varrho}_k(t) = \frac{1}{D} \sum_{n=0}^{D-1} \varrho_n(t) \text{tr}[\sigma_k^\dagger \mathfrak{L}[\sigma_n]], \quad (\text{A.5})$$

where we assume that $\mathfrak{L}[\bullet]$ is a linear superoperator. Note that if we identify the coefficient $\text{tr}[\sigma_k^\dagger \mathfrak{L}[\sigma_n]]/D$ in the above equation as an element at k -th row and n -th column of a $(D^2 \times D^2)$ -dimensional matrix \mathbb{L} , one can write

$$|\dot{\rho}(t)\rangle\rangle = \mathbb{L}|\rho(t)\rangle\rangle, \quad (\text{A.6})$$

where $|\rho(t)\rangle\rangle$ is a D^2 -dimensional vector with components $\varrho_n(t) = \text{tr}[\rho(t) \sigma_n^\dagger]$, $n = 0, 1, \dots, D-1$.

In particular, for the single-qubit case of interest here $D = 4$, and it means that

$$|\rho(t)\rangle\rangle = [1 \ \varrho_x(t) \ \varrho_y(t) \ \varrho_z(t)], \quad (\text{A.7})$$

where all dynamics of the system is mainly ruled by the three last elements of $|\rho(t)\rangle\rangle$. This information is important and we will mention it again soon. In an analogous way to the coherence vector $\vec{\varrho}(t)$ of the two-level system, we will call $|\rho(t)\rangle\rangle$ the *coherence supervector*.

Appendix A.2. The superoperator spectrum

As an important remark, this change of formalism has a price to be paid, and it is mainly due to the non-Hermiticity of the superoperator \mathbb{L} . Nevertheless, non-Hermitian operators can always be written in the Jordan canonical form, where $\mathbb{L}(t)$ displays a block-diagonal structure $\mathbb{L}_J(t)$ composed by Jordan blocks $J_n(t)$ associated with different time-dependent eigenvalues $\lambda_\alpha(t)$ of $\mathbb{L}(t)$ [40]. When such a Jordan decomposition is possible, we can write the diagonal form of the superoperator \mathbb{L} as

$$\mathbb{L}_J = \begin{bmatrix} J_{k_1}[\lambda_{k_1}] & 0 & 0 & \cdots & 0 \\ 0 & J_{k_2}[\lambda_{k_2}] & 0 & \cdots & 0 \\ \vdots & \ddots & \ddots & \ddots & \vdots \\ 0 & \cdots & 0 & \ddots & 0 \\ 0 & \cdots & \cdots & 0 & J_{k_N}[\lambda_N] \end{bmatrix}_{K \times K}, \quad (\text{A.8})$$

where N is the number of distinct eigenvalues $\lambda_\alpha(t)$ of $\mathbb{L}(t)$ and each block $J_{k_\alpha}[\lambda_\alpha(t)]$ is a $(k_\alpha \times k_\alpha)$ -dimensional matrix given as

$$J_k[\lambda_k] = \begin{bmatrix} \lambda_k & 1 & 0 & \cdots & 0 \\ 0 & \lambda_k & 1 & \cdots & 0 \\ \vdots & \ddots & \ddots & \ddots & \vdots \\ 0 & \cdots & 0 & \lambda_k & 1 \\ 0 & \cdots & \cdots & 0 & \lambda_k \end{bmatrix}_{k \times k}, \quad (\text{A.9})$$

with λ_k denoting the eigenvalues of \mathbb{L} . Since the Hilbert space of the system has dimension D , one finds $k_1 + k_2 + \cdots + k_N = D^2$. In addition, as an immediate consequence of the structure of $\mathbb{L}_J(t)$, one see that $\mathbb{L}(t)$ does not admit the existence of eigenvectors. Instead eigenvectors, we define *right* $|\mathcal{R}_\alpha^{n_\alpha}\rangle\rangle$ and *left quasi*-eigenvectors $\langle\langle \mathcal{L}_\alpha^{n_\alpha} |$ of \mathbb{L} associated with the eigenvalue λ_α , satisfying

$$\mathbb{L}|\mathcal{R}_\alpha^{n_\alpha}\rangle\rangle = |\mathcal{R}_\alpha^{(n_\alpha-1)}\rangle\rangle + \lambda_\alpha|\mathcal{R}_\alpha^{n_\alpha}\rangle\rangle, \quad (\text{A.10})$$

$$\langle\langle \mathcal{L}_\alpha^{n_\alpha} | \mathbb{L} = \langle\langle \mathcal{L}_\alpha^{(n_\alpha+1)} | + \langle\langle \mathcal{L}_\alpha^{n_\alpha} | \lambda_\alpha. \quad (\text{A.11})$$

The set $\{|\mathcal{R}_\alpha^{n_\alpha}\rangle\rangle\}$ combined with $\{\langle\langle \mathcal{L}_\alpha^{n_\alpha} |\}$ constitutes a basis for the space associated with the operator $\mathbb{L}(t)$ and satisfies the normalization condition $\langle\langle \mathcal{L}_\beta^{m_\beta} | \mathcal{R}_\alpha^{n_\alpha}\rangle\rangle = \delta_{\beta\alpha} \delta_{m_\beta n_\alpha}$ and completeness relation

$$\sum_{\alpha=1}^N \sum_{n_\alpha=1}^{N_\alpha} |\mathcal{R}_\alpha^{n_\alpha}\rangle\rangle \langle\langle \mathcal{L}_\alpha^{n_\alpha} | = \mathbb{1}_{D^2 \times D^2}, \quad (\text{A.12})$$

where N is the number of Jordan blocks in Eq. (A.8) and N_α is the dimension of the α -th Jordan block.

In particular (for the case of interest here), for the cases in which the spectrum of $\lambda_\alpha(t)$ is non-degenerate, we can write the uni-dimensional Jordan block decomposition ($N_\alpha = 1, \forall \alpha$) from the eigenvector equations written as

$$\mathbb{1}|\mathcal{R}_\alpha\rangle\rangle = \lambda_\alpha|\mathcal{R}_\alpha\rangle\rangle, \quad \langle\langle\mathcal{L}_\alpha|\mathbb{1} = \langle\langle\mathcal{L}_\alpha|\lambda_\alpha. \quad (\text{A.13})$$

and then

$$\sum_{\alpha=1}^N |\mathcal{R}_\alpha\rangle\rangle\langle\langle\mathcal{L}_\alpha| = \mathbb{1}_{D^2 \times D^2}. \quad (\text{A.14})$$

Appendix B. Superoperator formalism and Mpemba effect

In this section we explain how the emergence of Mpemba effect observed in the system considered in the main text can be explained using the superoperator formalism. To this end, we move our description to the superoperator formalism, where the system evolution can be properly described by Eq. (A.6). In this formalism, we can write the solution for the Schrödinger-like equation as

$$|\psi(t)\rangle\rangle = e^{\mathbb{L}t}|\psi(0)\rangle\rangle \quad (\text{B.1})$$

where \mathbb{L} is the superoperator. In particular, using Eq. (A.14), it is convenient to write the initial state as a superposition of the right eigenvectors $|\mathcal{R}_n\rangle\rangle$ of \mathbb{L} as

$$|\psi(0)\rangle\rangle = \left[\sum_n |\mathcal{R}_n\rangle\rangle\langle\langle\mathcal{L}_n| \right] |\psi(0)\rangle\rangle = \sum_n \left[\langle\langle\mathcal{L}_n|\psi(0)\rangle\rangle \right] |\mathcal{R}_n\rangle\rangle = \sum_n c_n^L |\mathcal{R}_n\rangle\rangle, \quad (\text{B.2})$$

with $c_n^L = \langle\langle\mathcal{L}_n|\psi(0)\rangle\rangle$ the ‘‘projection’’ of the initial state in the left eigenvector basis of \mathbb{L} . In this way, we can write that

$$|\psi(t)\rangle\rangle = e^{\mathbb{L}t}|\psi(0)\rangle\rangle = \sum_n c_n^L e^{\mathbb{L}t} |\mathcal{R}_n\rangle\rangle = \sum_n c_n^L e^{\lambda_n t} |\mathcal{R}_n\rangle\rangle, \quad (\text{B.3})$$

where we can explicitly write the steady-state component of the system (associated to $\lambda_0 = 0$) in this equation as

$$|\psi(t)\rangle\rangle = c_0^L |\mathcal{R}_0\rangle\rangle + \sum_{n \neq 0} c_n^L e^{\lambda_n t} |\mathcal{R}_n\rangle\rangle, \quad (\text{B.4})$$

Therefore, for a run time large enough we get the steady-state approximation

$$|\psi(t)\rangle\rangle \approx c_0^L |\mathcal{R}_0\rangle\rangle, \quad (\text{B.5})$$

because $\text{Re}[\lambda_n] < 0$, and therefore we can observe the emergence of the Mpemba effect only considering the time-dependent term in equation above. In this way, we establish some sufficient conditions to observe *strong* Mpemba effect. By ordering $\text{Re}[\lambda_1] \leq \text{Re}[\lambda_2] \leq \text{Re}[\lambda_3]$, we have the conditions to be satisfied for the hot initial state $|\psi_{\text{hot}}(0)\rangle\rangle$

$$|c_3^{L,\text{hot}}| < |c_2^{L,\text{hot}}| < |c_1^{L,\text{hot}}|, \quad (\text{B.6})$$

with $c_n^{L,\text{hot}} = \langle\langle\mathcal{L}_n|\psi_{\text{hot}}(0)\rangle\rangle$, and the cold state satisfies

$$|c_3^{L,\text{cold}}| > |c_2^{L,\text{cold}}| > |c_1^{L,\text{cold}}|. \quad (\text{B.7})$$

with $c_n^{L,\text{cold}} = \langle\langle\mathcal{L}_n|\psi_{\text{cold}}(0)\rangle\rangle$. Any other combination will provide a moderate Mpemba effect.

References

- [1] E. B. Mpemba and D. G. Osborne, *Physics Education* **4**, 172 (1969).
- [2] F. Carollo, A. Lasanta, and I. Lesanovsky, *Phys. Rev. Lett.* **127**, 060401 (2021).
- [3] A. K. Chatterjee, S. Takada, and H. Hayakawa, *Phys. Rev. Lett.* **131**, 080402 (2023).
- [4] C. Rylands *et al.*, arXiv e-prints, arXiv:2310.04419 (2023), 2310.04419.
- [5] S. Kochsiek, F. Carollo, and I. Lesanovsky, *Phys. Rev. A* **106**, 012207 (2022).
- [6] F. Ares, S. Murciano, and P. Calabrese, *Nature Communications* **14**, 2036 (2023).
- [7] M. Moroder, O. Culhane, K. Zawadzki, and J. Goold, arXiv e-prints, arXiv:2403.16959 (2024), 2403.16959.
- [8] S. K. Manikandan, *Phys. Rev. Res.* **3**, 043108 (2021).
- [9] F. Ivander, N. Anto-Sztrikacs, and D. Segal, *Phys. Rev. E* **108**, 014130 (2023).
- [10] A. K. Chatterjee, S. Takada, and H. Hayakawa, arXiv e-prints, arXiv:2311.01347 (2023), 2311.01347.
- [11] S. Liu, H.-K. Zhang, S. Yin, and S.-X. Zhang, arXiv e-prints, arXiv:2403.08459 (2024), 2403.08459.
- [12] X. Turkeshi, P. Calabrese, and A. De Luca, arXiv e-prints, arXiv:2405.14514 (2024), 2405.14514.
- [13] S. Murciano, F. Ares, I. Klich, and P. Calabrese, *Journal of Statistical Mechanics: Theory and Experiment* **2024**, 013103 (2024).
- [14] S. Yamashika, F. Ares, and P. Calabrese, *Phys. Rev. B* **110**, 085126 (2024).
- [15] J. Zhang *et al.*, arXiv e-prints, arXiv:2401.15951 (2024), 2401.15951.
- [16] M. S. Sarandy and D. A. Lidar, *Phys. Rev. Lett.* **95**, 250503 (2005).
- [17] K. McKenzie, D. A. Shaddock, D. E. McClelland, B. C. Buchler, and P. K. Lam, *Phys. Rev. Lett.* **88**, 231102 (2002).
- [18] H. Vahlbruch *et al.*, *Classical and Quantum Gravity* **27**, 084027 (2010).
- [19] Ligo Scientific Collaboration *et al.*, *Nature Physics* **7**, 962 (2011).
- [20] P. M. Anisimov *et al.*, *Phys. Rev. Lett.* **104**, 103602 (2010).
- [21] S. Steinlechner *et al.*, *Nature Photonics* **7**, 626 (2013).
- [22] J. Klaers, S. Faelt, A. Imamoglu, and E. Togan, *Phys. Rev. X* **7**, 031044 (2017).
- [23] D. von Lindenfels *et al.*, *Phys. Rev. Lett.* **123**, 080602 (2019).
- [24] Y. Xiao *et al.*, *Phys. Rev. Res.* **5**, 043185 (2023).
- [25] W. Niedenzu, V. Mukherjee, A. Ghosh, A. G. Kofman, and G. Kurizki, *Nature communications* **9**, 165 (2018).
- [26] S. Roman, *Physics Reports* **684**, 1 (2017), Squeezed states of light and their applications in laser interferometers.
- [27] M. A. Nielsen and I. L. Chuang, *Quantum Computation and Quantum Information: 10th Anniversary Edition*, 10th ed. (Cambridge University Press, New York, NY, USA, 2011).
- [28] M. S. Sarandy and D. A. Lidar, *Phys. Rev. A* **71**, 012331 (2005).
- [29] A. C. Santos and M. S. Sarandy, *Phys. Rev. A* **102**, 052215 (2020).
- [30] R. Alicki and K. Lendi, *Recent Developments* (Springer Berlin Heidelberg, Berlin, Heidelberg, 2007), pp. 109–121.
- [31] H.-P. Breuer and F. Petruccione, *The Theory of Open Quantum Systems* (Cambridge University Press, Oxford University Press, Oxford, UK, 2007).
- [32] R. E. Slusher, L. W. Hollberg, B. Yurke, J. C. Mertz, and J. F. Valley, *Phys. Rev. Lett.* **55**, 2409 (1985).
- [33] A. Ourjoumtsev *et al.*, *Nature* **474**, 623 (2011).
- [34] J. Heinze, B. Willke, and H. Vahlbruch, *Phys. Rev. Lett.* **128**, 083606 (2022).
- [35] G. Manzano, *Phys. Rev. E* **98**, 042123 (2018).
- [36] Z. F. B. J. Dalton and S. Swain, *Journal of Modern Optics* **46**, 379 (1999).
- [37] S. Banerjee, V. Ravishankar, and R. Srikanth, *Annals of Physics* **325**, 816 (2010).
- [38] R. Srikanth and S. Banerjee, *Phys. Rev. A* **77**, 012318 (2008).
- [39] A. C. Santos and M. S. Sarandy, *Phys. Rev. A* **104**, 062421 (2021).
- [40] R. A. Horn and C. R. Johnson, *Matrix analysis*, Second ed. (Cambridge University Press, Cambridge, 2012).